



Article

Quantification of Cycling Smoothness in Children with Cerebral Palsy

Ahad Behboodi ^{1,*}, Ashwini Sansare ^{2,†} and Samuel C. K. Lee ²¹ Rehabilitation Medicine Department, Clinical Center, National Institutes of Health, Bethesda, MD 20892, USA² Department of Physical Therapy, University of Delaware, Newark, DE 19713, USA

* Correspondence: ahadbeh@udel.edu

† These authors contributed equally to this work.

Abstract: Smoothness is a hallmark of skilled, coordinated movement, however, mathematically quantifying movement smoothness is nuanced. Several smoothness metrics exist, each having its own limitations and may be specific to a particular motion such as upper limb reaching. To date, there is no consensus on which smoothness metric is the most appropriate for assessing cycling motion in children with cerebral palsy (CP). We evaluated the ability of four preexisting metrics, dimensionless jerk, spectral arc length measure, roughness index, and cross-correlation; and two new metrics, arc length and root mean square error, to quantify the smoothness of cycling in a preexisting dataset from children with CP (mean age 13.7 ± 2.6 years). First, to measure the repeatability of each measure in distinguishing between different levels of un-smoothness, we applied each metric to a set of simulated crank motion signals with a known number of aberrant revolutions using subjects' actual crank angle data. Second, we used discriminant function analysis to statistically compare the strength of the six metrics, relative to each other, to discriminate between a smooth cycling motion obtained from a dataset of typically developed children (TD), the control group (mean age 14.9 ± 1.4 years), and a less smooth, halted cycling motion obtained from children with CP. Our results show that (1) ArcL showed the highest repeatability in accurately quantifying an unsmooth motion when the same cycling revolutions were presented in a different order, and (2) ArcL and DJ had the highest discriminatory ability to differentiate between an unsmooth and smooth cycling motion. Combining the results from the repeatability and discriminatory analysis, ArcL was the most repeatable and sensitive metric in identifying unsmooth, halted cycling motion from smooth motion. ArcL can hence be used as a metric in future studies to quantify changes in the smoothness of cycling motion pre- vs. post-interventions. Further, this metric may serve as a tool to track motor recovery not just in individuals with CP but in other patient populations with similar neurological deficits that may present with halted, unsmooth cycling motion.

Keywords: roughness index; spectral arc length; cycling rhythm; cycling biomechanics; cerebral palsy; smoothness



Citation: Behboodi, A.; Sansare, A.; Lee, S.C.K. Quantification of Cycling Smoothness in Children with Cerebral Palsy. *Biomechanics* **2023**, *3*, 79–92. <https://doi.org/10.3390/biomechanics3010008>

Academic Editors: Urs Granacher and Katherine Boyer

Received: 10 October 2022

Revised: 21 December 2022

Accepted: 13 January 2023

Published: 6 February 2023



Copyright: © 2023 by the authors. Licensee MDPI, Basel, Switzerland. This article is an open access article distributed under the terms and conditions of the Creative Commons Attribution (CC BY) license (<https://creativecommons.org/licenses/by/4.0/>).

1. Introduction

Cerebral palsy (CP) is a non-progressive disorder of movement and posture that results from an injury to the infant or fetal brain, resulting in impaired sensorimotor coordination and/or regulation of muscle tone [1]. Individuals with CP typically present with reduced muscle strength [2] muscle tone abnormalities, co-contraction of agonist and antagonist muscle groups [3–5], and poor selective voluntary motor control [6]. Recumbent stationary cycling is a safe and practical exercise modality for those lacking the dynamic postural control and strength necessary for exercising in an upright position. Cycling has shown therapeutic benefits in patients with stroke [7,8] and children with CP [9].

Muscle co-contraction and altered motor control characteristics of children with CP, however, contribute to irregular and halted progression of cycling crank revolution resulting in poor smoothness of cycling. Smooth movements are an attribute of a well-developed

motor control [10]; accordingly, smoothness of upper limb movement is used as a marker of motor recovery in patients with stroke [11]. Thus, the need for quantification of movement smoothness to assess motor learning and recovery has resulted in various metrics to quantify different aspects of a movement's profile [12]; nonetheless, the utility of such measures are mixed even when unsmooth movements are obviously present [13].

Although smoothness is regarded as a hallmark of skilled and coordinated movement, and despite the importance of cycling interventions in rehabilitation, there are limited studies on quantifying the smoothness of cycling, especially in the CP population. Thus, to track motor recovery in children with CP following cycling training protocols, a sensitive metric to quantify cycling smoothness is essential. To find such a metric, we evaluated three conventional, one recently proposed in our previous work, and two new metrics proposed here, with our CP cycling data set.

While smoothness is an intuitive concept, it requires a precise mathematical and numerical method for its quantification. Balasubramanian et al. [14] introduced a systematic approach to identify an appropriate smoothness metric for assessing sensorimotor impairment and motor learning. Intuitively, a desirable metric will measure the shape of motion independent of its duration and amplitude [13,14]. In addition, Balasubramanian et al. suggested that a reliable metric must be sensitive to changes in movement parameters within the physiological range, and it must be robust and computationally inexpensive for practical implementation [14]. Therefore, we compared the ability of the following six potential metric candidates that have the desired characteristics to quantify cycling crank angle smoothness: dimensionless jerk [13]; spectral arc length metric (SALM) [14]; roughness index (RI) [15]; cross-correlation (Xcorr) [16]; arc length (ArcL); and root mean square error (RMSE).

Jerk, the time-derivative of acceleration, has been used to quantify smoothness, as a measure of motor control, in patients with Parkinson's Disease [17,18], Huntington's Disease [19], and post-stroke populations [20]. Being independent of amplitude and duration of motion, unlike most other jerk-based measures, dimensionless jerk (DJ), proposed by Hogan et al. [13], and its logarithmic version, proposed by Balasubramanian et al. [12] have shown more sensitivity, reliability, and robust assessment in comparison to the other jerk-based smoothness metrics.

SALM is the arc length of the envelope of the speed profile in the frequency domain. It demonstrated promising results in quantifying the smoothness of upper extremity reaching motion in children with CP [21,22]. SALM was used successfully to classify upper extremity motion in-patient with neurological disorders ($n = 10$) into five levels of motor impairments [23].

The capability of DJ and SALM in measuring the smoothness of upper extremity motion was evaluated against other smoothness measures in individuals with stroke [12] and CP [22]. Balasubramanian et al. compared the number of peaks, local maxima, in the speed profile of the motion, root mean squared jerk, normalized mean absolute jerk, DJ, speed ArcL, and SALM [12]. They measured the smoothness of the upper extremity reaching motion in two post-stroke survivors and one healthy adult, and in simulated data, finding that SALM is the most robust metric in the presence of noise, inter-submovement intervals, and motion arrest. SALM was the most sensitive metric in quantifying improved smoothness of arm motion in stroke population; speed profile ArcL and DJ were the closest competitors to SALM Quijano-González et al. [22] and Rincón Montes et al. [21] evaluated DJ, SALM, and numbers of motion peaks in distinguishing upper extremity motion of children with CP ($n = 3$ for Rincón Montes et al., $n = 10$ for Quijano-Gonzalez et al.) and typically developing peers. Both studies demonstrated the SALM and DJ could differentiate between CP and TD motion and for affected and less-affected sides in subjects with CP, with SALM showing more sensitivity. Logarithmic DJ and SALM surpass the number of local peaks in the speed profile, in all of the aforementioned studies; thus, the number of peaks method was not included in our evaluation.

Speed profile's ArcL, i.e., the arc length of the speed signal, also showed a high level of sensitivity and reliability in comparisons by Balasubramanian et al. [12]. We included a modified version of the speed ArcL in our comparison; instead of measuring the arc length of the speed profile as proposed by Balasubramanian, we used the crank angle's arc length, i.e., the arc length of the position profile.

Chen et al., pioneers in measuring cycling smoothness in rehabilitation applications, proposed the roughness index, RI, for quantifying the smoothness of cycling in post-stroke survivors. The RI uses the curvature of the instantaneous crank speed, revolution per minute (RPM), to measure the cycling smoothness [15]; the lower the RI indicates the greater smoothness of the cycling motion. The RI metric was mostly used to characterize cycling in the population with stroke [15] or to quantify the effects of the functional electrical stimulation [24], visual feedback [25], or maximal workload [26] on cycling performance.

XCorr was used as a measure of the similarity between the two signals [27,28] by comparing the ideal crank rotation in a cycling system to the observed crank rotation in the sagittal plane. When used as a smoothness metric, the higher the XCorr factor, the greater the similarity of the subject's crank motion to the ideal crank motion. In a study conducted by Sansare et al. [16], XCorr could successfully differentiate the cycling smoothness of children with CP and typical development (TD ($p < 0.0001$)). To further evaluate this metric, XCorr is included in our comparison to assess its performance in comparison with the described metrics. We also propose another intuitive metric called RMSE, which is the root mean square error (RMSE) between the subject's crank motion and the ideal crank motion.

The objective of this study was to compare the repeatability and sensitivity of six different smoothness metrics in distinguishing between different levels of un-smoothness in cycling data from children with CP. To this end, we followed a two-fold approach; first, to measure the repeatability of each measure in distinguishing between different levels of noise, as representations of un-smoothness. Second, we used discriminant function analysis to statistically compare the strength of the six metrics relative to each other to discriminate between a smooth cycling motion obtained from a dataset of typically developed children (TD), and less smooth, halted cycling motions obtained from children with CP.

2. Materials and Methods

2.1. Participants

CP group: the CP data set is from a larger study. Thirty-one ambulatory adolescents with CP (mean age 13.7 ± 2.6 years, 6 females) with gross motor function classification system (GMFCS) [29] levels II-IV were recruited through the outpatient CP clinic at Shriners Hospital for Children, Philadelphia, and local referral sources. Institutional Review Board approval and informed consent and assent were obtained. All subjects with CP underwent screening by a physical therapist for the inclusion and exclusion criteria specified in Table 1. There were no criteria for the weight of participants. The result of the cycling intervention is previously published by our group [30]. Here, we used the crank angles collected from one of the cohort groups in the study, only to assess the capabilities of the aforementioned metrics in quantifying smoothness when subjects did not cycle smoothly.

Control group (TD): The data from TD controls were obtained from a pre-existing dataset of healthy, typically developing children (mean age 14.9 ± 1.4 years, 7 females). TD datasets were obtained from a larger study [31]. The inclusion criteria were (1) age (13–19 years); (2) the ability to maintain a sitting position; (3) a minimum of 15° of plantarflexion range of motion [31].

2.2. Data Collection

A commercially available recumbent sport tricycle (www.kmxkarts.co.uk) fitted with shank guide orthoses to control for excess hip adduction and abduction movement, was used for the CP group (Figure 1A) [32]. The TD group used a semi-recumbent, free-standing Restorative Therapies, Inc. bicycle (Baltimore, MD) attached to a therapy bench (Figure 1B). Despite the different cycling systems for CP and TD groups, anthropometric differences

of individuals within and across groups were minimized by standardizing positioning in both cycling setups (Figure 1C). Additionally, the force transducer pedals used for the TD group by Johnston et al., [31] also used on the recumbent tricycle used for the CP group in Sansare et al. [16,30], which further standardized foot and shank positioning across the two datasets. The bicycle crank and spindle assembly for both systems were instrumented with sensors to indicate crank position and cadence. Both groups cycled for three trials of 15–30 s, depending on their capabilities. Data were analyzed using customized software (MATLAB The Mathworks, Inc., Natick, MA, USA). Note that, here we used the TD dataset, from Johnston et al. [31], as the representative dataset of smooth cycling, and the CP dataset, from Sansare et al. [30], was used as the representative dataset of unsmooth cycling. The crank angle data from the CP group were visually less smooth when compared with those of TD group. The focus of this paper is comparison between six different types of smoothness metrics and not comparison between CP versus TD groups. The result of cycling intervention on CP and comparison between CP and TD groups were published in Sansare et al. [30], and Johnston et al. [31], respectively.

Table 1. Inclusion criteria.

Inclusion Criteria	Exclusion Criteria
<p>Ages 10–18. Diagnosis of spastic CP.</p> <p>GMFCS II, III, or IV. Adequate range of motion of the hips, knees, and ankles to allow pedaling. Visuoperceptual skills and cognitive/communication skills to follow multiple-step commands for attending to exercise and data collection. Ability to communicate pain or discomfort with testing and training procedures.</p>	<p>Lower-extremity orthopedic surgery or traumatic fracture within the past 6 months.</p> <p>Lower-extremity joint pain during cycling. Spinal fusion extending to the pelvis. Hip, knee, or ankle joint instability or dislocation. Lower-limb stress fractures in the past year. Symptomatic or current diagnosis of cardiac disease as assessed by the American Heart Association guidelines for cardiac history. Current pulmonary disease or asthma and taking oral steroids or hospitalized for an acute episode in the past 6 months. Severe spasticity in legs (score of 4 on the Modified Ashworth Scale). Severely limited joint range of motion or irreversible muscle contractures that prevented safe positioning on the cycle. Diagnosis of athetoid or ataxic CP. Less than six months following Botox injections to the leg muscles.</p>

2.3. Data Analysis

We discarded the first and the last revolution of the crank angle to minimize the effects of acceleration and deceleration, respectively. Crank angle data were low-pass filtered at 5 Hz (4th order Butterworth) and plotted against time, resulting in a sawtooth waveform indicating the angle of the recumbent cycle's crank as the trial progressed. Five Hz frequency was chosen by Frequency power analysis of the *crankIS*. There is a discontinuity in the crank angle as it crosses from $360^\circ \rightarrow 0^\circ$ (Figure 2A [16]), i.e., as it transitions from the end of one revolution to beginning of the next revolution. To eliminate this discontinuity, we converted the crank angle to a linear form by concatenating the angle data in series. The resultant angle-in-series data (*crankIS*) thus consists of a time series representing the angular progression of the crank from zero to $N \times 360^\circ$, where N is the number of revolutions (Figure 2B [16]). To quantify the deviation of each subject's *crankIS* from the theoretically smooth crank angle, the ideal crank angle (*crankIDL*), was defined as the straight line that connected the beginning to the end of angle-in-series data points. This straight line accounted for the subject-specific cycling duration; however, note that this ideal scenario is not practically achievable as there are acceleration and deceleration

segments in subjects' crank-in-series, no matter how smooth they are, resulting in an S-shape trajectory for any subject. The first derivative of the *crankIS* was used to measure the instantaneous RPM (*crankRPM*). See Table 2 for the summary of the terms.

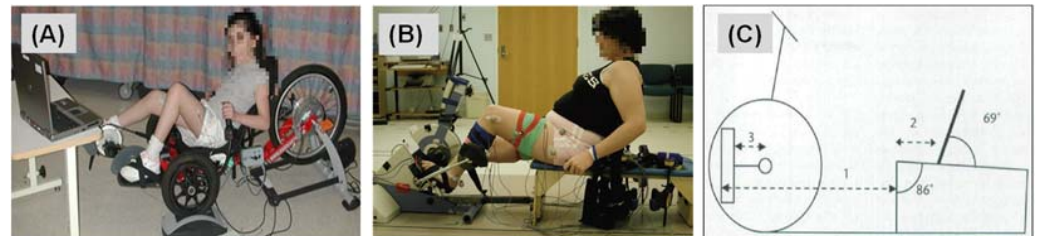


Figure 1. Recumbent cycling setup. (A) the set-up for the CP group. (B) semi-recumbent set-up used in the TD group. (C) Adjusted components in both set-ups based on subject anthropometrics. (1) Seat-to-pedal distance = 85% of the distance from the greater trochanter to the base of the calcaneus. (2) Seat-to-greater trochanter distance = 15% of the distance from the greater trochanter to the base of the calcaneus. (3) Crank arm length = 30% of tibial length. The seat back of (C) emulated the angle of the recumbent cycle seat of (A) and was placed comfortably behind the subject while maintaining the seat to greater trochanter distance.

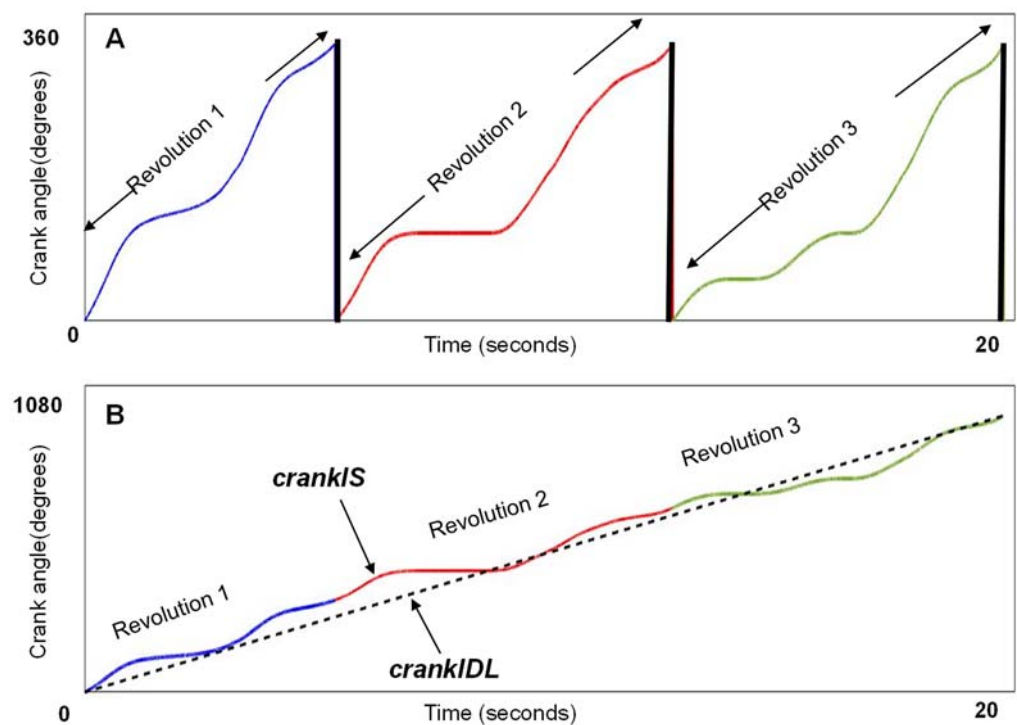


Figure 2. Schematic representation of crank angle smoothness. (A) Depicts crank angle (plotted against time in seconds) for 3 representative revolutions from a child with CP, each color depicting one revolution from 0° to 360° , thick vertical black lines indicate the discontinuity between 360° and 0° at the end of each revolution. (B) Depicts the concatenation of the three revolutions resulting in a time series, *crankIS*, representing the angular progression of the crank from zero to 3×360 . The dash line is the hypothetical smoothest progress of crank, *crankIDL* [16].

Table 2. Summary of the terms.

crankIS	A line form by concatenating the angle data of each revolution in series
crankRPM	The instantaneous RPM of crankIS
crankIDL	That connected the beginning to the end of angle-in-series data points
crankSim	The simulated crankIS using the aberrant revolutions of CP subjects

2.4. Smoothness Metrics

DJ. To measure DJ, the crank-in-series jerk, the third derivative, was squared and integrated over time. The dimension of this integration is length squared over the 5th power of time. Thus, to become dimensionless, DJ was defined by Equation (1) [13]:

$$DJ = \left(\sum_{n=0}^{N \times 360^\circ} \text{crankRPM}''(n) \right) D^5 / A^2 \quad (1)$$

where N is number of revolutions, D is the duration, and A is the amplitude of *crankIS*. To smooth the jerk signal, it was low passed filtered ($f_c = 5$ Hz, 4th order Butterworth) using MATLAB's zero-phase digital filter, *filtfilt*. The filtering was in addition to the preprocessing of the *crankIS*.

SALM is defined as the arc length of the *crankRPM*'s envelope in the frequency domain, i.e., the envelope is its Fourier spectrum magnitude [14]. The frequency range to measure SALM is defined based on the target motion using user-defined parameters [14].

ArcL is defined as the length of the *crankIS* curvature. The result of preliminary statistical analysis showed there was no significant difference between measuring ArcL of the speed profile, *crankRPM*, as suggested by Balasubramanian et al. [12], and measuring ArcL of *crankIS*, in our application. Therefore, we chose the simpler approach, ArcL of *crankIS*. This metric was then normalized to the length of the *crankIDL*, calculated using the Pythagorean theorem.

RI was defined as the curvature of the six-order polynomial curve fitted to the *crankRPM*, using the Equation (2) [15]:

$$RI = \sum_{n=0}^{N \times 360^\circ} |d\text{crankRPM}/ds| \quad (2)$$

where s is the crank angle.

XCorr was defined as the maximum of the cross-correlation of the *crankIS* and *crankIDL*. To make XCorr dimensionless, the maximum of cross-correlation was normalized to the maximum of *crankIDL*'s autocorrelation, the cross-correlation of the signal with itself. The results were expressed as a smoothness metric. Further detail on XCorr can be found in study by Sansare et al. introducing this metric [16].

RMSE was defined as the RMSE between the *crankIS* and the *crankIDL*.

For all the aforementioned metrics the lower the outcome the smoother the cycling.

2.5. Simulated Signals Using Real Aberrant Cycles

To objectively quantify the increasing level of un-smoothness, three aberrant revolutions from CP subjects' crank angles were used to generate *crankIS* simulations. A physical therapist visually inspected the CP subjects' crank angles and extracted three revolutions that consistently represented aberrant patterns in multiple subjects. These patterns showed different levels of un-smoothness, (Figure 3). The chosen revolutions were interpolated to 12 k samples. Six simulated signals were then generated by randomly replacing the revolutions of a *crankIDL* ($N = 6$ revolutions, $A = 2160^\circ$, 10 rpm, and 2 kHz sampling frequency) with the three aberrant revolutions (Figure 3). We call these simulated signals *crankSims*. The detailed description of *crankSims* is as follow:

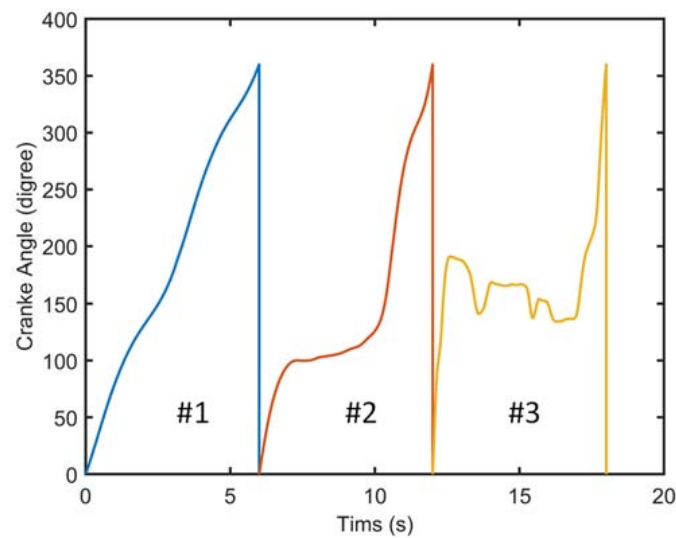


Figure 3. Three aberrant revolutions. Aberrant revolution #1 (blue) #2 (orange) #3 (yellow).

crankSim1: aberrant revolution #1 (Figure 3) randomly replaced a revolution in the *crankIDL*. **crankSim2:** aberrant revolution #1 randomly replaced two revolutions in the *crankIDL*. **crankSim3:** aberrant revolution #1 randomly replaced two revolutions in *crankIDL* and revolution #2 randomly replaced one revolution. **crankSim4:** aberrant revolutions #1 and #2 randomly replaced 2 revolutions, each. **crankSim5:** aberrant revolutions #1 and #2 randomly replaced two revolutions in *crankIDL* each, and revolution #3 randomly replaced one revolution. **crankSim6:** aberrant revolutions #1, #2, and #3 randomly replaced 2 revolutions of *crankIDL*, each.

The repetition of aberrant revolutions in the *crankSim* 2, 4, and 6, is to evaluate the sensitivity of the metrics to an equal amount of increasing un-smoothness using the same aberrant revolution used in the previous *crankSim*, i.e., *crankSims* 1, 3, 5.

The *crankSims* are depicted in Figure 4.

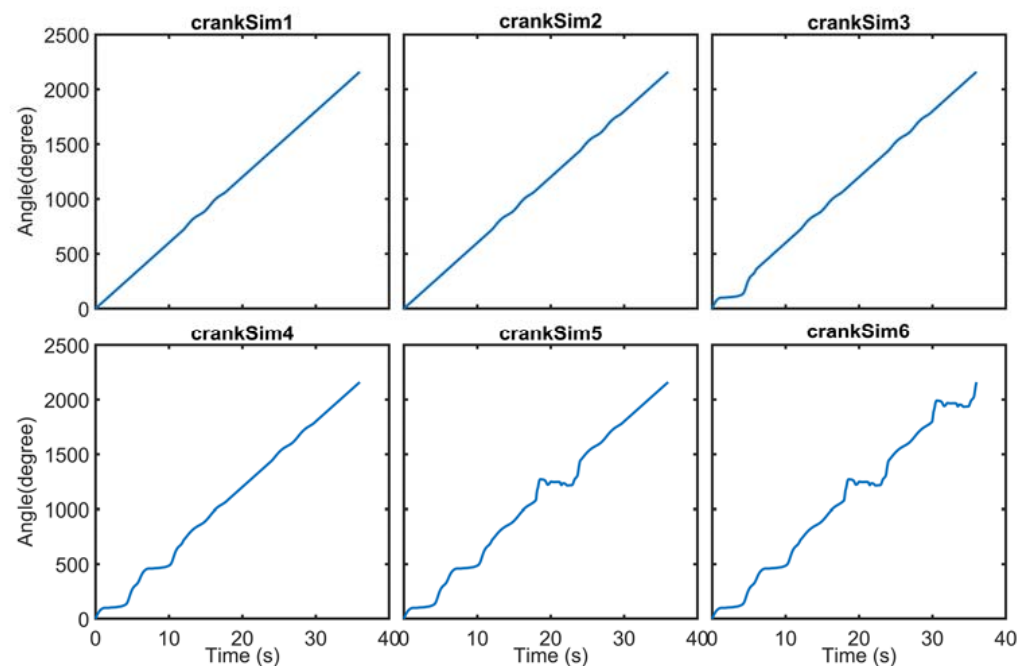


Figure 4. Crank simulation with different levels of un-smoothness, *crankSims*.

To evaluate the repeatability of the metrics in differentiating between various levels of un-smoothness, we shuffled the order of revolutions of each *crankSims* five times, resulting in five sets of *crankSims*. We used each of the six metrics to then compute the smoothness of the *crankSims* of each set, depicted with different colors in each panel of Figure 5. Therefore, we have five values for each *crankSims*, and ideally, the shuffling should result in a similar smoothness value calculated by each metric.

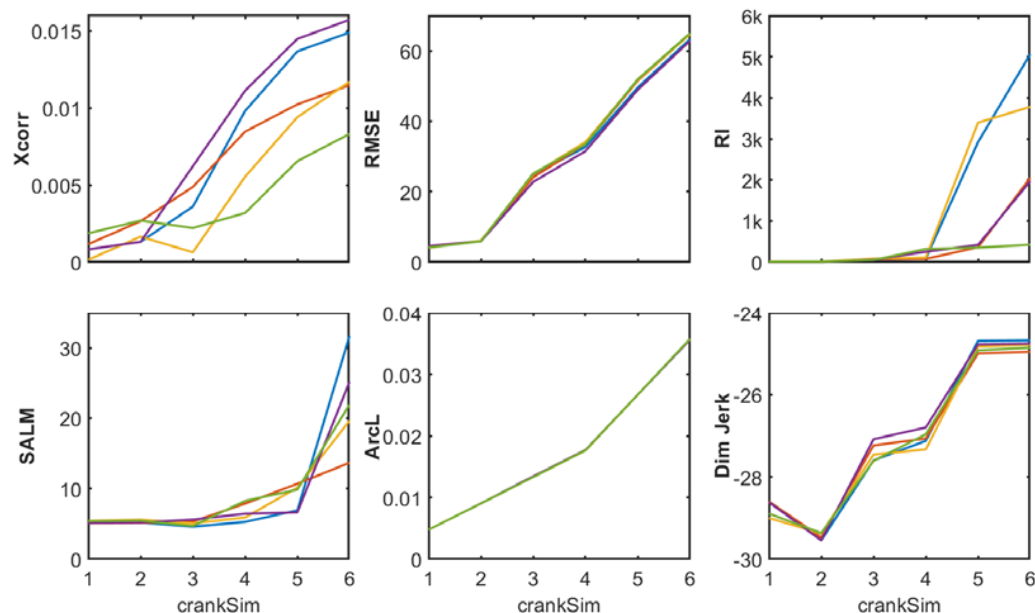


Figure 5. The repeatability of the metrics in differentiating between various levels of un-smoothness, each color represents the output of each metric (XCorr, RMSE, RI, SALM, ArcL, and DJ) in quantifying the un-smoothness level of each set of crankSims, crankSims1 to 6.

2.6. Statistical Analysis

We evaluated the diagnostic (discriminant) validity of the six different smoothness metrics for evaluating cycling smoothness in two groups: children with CP and those with typical development TD. Dependent variables were the six different metrics: DJ, SALM, ArcL, RI, Xcorr, and RMSE.

Data were analyzed using a one-way between-subjects multivariate analysis of variance (MANOVA). Secondary analyses used a direct-entry (simultaneous) discriminant function analysis (DFA) to evaluate the relative strength of each dependent variable (DJ, SALM, ArcL, RI, Xcorr, and RMSE) in discriminating between the TD and CP cycling smoothness in comparison to each other. In essence, DFA results in a discriminant function that uses a combination of the dependent variables to maximize the separation between the two groups, in this case, the CP and TD cycling smoothness. The structure matrix from the DFA will be interpreted using the loadings, which are the correlations between each smoothness metric and the discriminant function. A larger loading implies a larger absolute correlation between the discriminant function and the variable and in turn implies a larger contribution to the discrimination between TD and CP cycling smoothness. Loadings above 0.71 are considered excellent, 0.71–0.63 are very good, 0.63–0.55 are good, 0.55–0.45 are fair, and below 0.45 are poor [33]. By ranking the metrics by their loadings, we were able to rank the metrics by their ability to distinguish between different smoothness levels during cycling. Finally, to cross-validate our results and to evaluate the accuracy of the DFA in predicting group membership, we performed a classification analysis after the DFA. That is, the classification analysis compared the “predicted group membership” based on the results from the DFA with the actual group membership as CP or TD to give a percentage of the correct classifications. Using the same sample that was used for the DFA for the classification analysis, however, might introduce a bias. To avoid this bias, the jack-knife

procedure [34], which resamples the data by sequentially leaving one observation out during each iteration of resampling, was used.

3. Results

Figure 5 demonstrates the repeatability of each metric. In the case of a metric with acceptable repeatability, first, we expect the colored lines to be very close to each other, i.e., show low variability at a similar level of un-smoothness resulting from shuffling the revolutions; in an ideal scenario, colored lines would overlap entirely, i.e., the metric outputs similar values for all five shuffling of each specific *crankSims*. Second, because the un-smoothness level increases by adding more aberrant cycles, we expected the output of each metric to increase, preferably linearly. ArcL, RMSE, and DJ satisfy both of the above expectations, i.e., each colored line has a similar value at each *crankSims* and shows an increase in the smoothness from *crankSims* 0 to 6 (Figure 5). DJ showed more variability between shufflings, in comparison with ArcL and RMSE; it could not maintain the desired linear ascending trend for *crankSim*2. Overall, ArcL demonstrated a linear increase in smoothness value as the *crankSims* became more unsmooth and the shuffling resulted in almost identical ARcL values. XCorr, RI, and SALM, however, showed a high level of variability at each *crankSims* and were unsuccessful in following the ascending trend.

Distributional statistics are presented separately for each group (Table 3). The MANOVA was significant (Pillai's Trace = 1.00, $F = 16611.935$, $df [6,34]$, $p < 0.001$), showing that the smoothness metrics were significantly affected by the membership in the CP or TD group. While the assumption of multivariate homogeneity among the covariance matrices was not satisfied, this problem was circumvented through the use of Pillai's trace [35].

Table 3. Cycling smoothness metrics for the CP and TD groups.

Cycling Smoothness	CP		TD	
	M	SD	M	SD
DJ	0.031	0.119	0.007	0.010
SALM	-2.871	0.428	-11.900	0.374
RI	5523.579	14,136.316	2.281	1.156
ArcL	-0.008	0.006	-0.997	0.001
XCorr	0.039	0.058	0.006	0.003
RMSE	120.165	155.602	4.298	1.804

Follow-up comparisons to MANOVA using DFA revealed a discriminant function that was statistically significant (Wilks $\Lambda < 0.001$, $\chi^2 = 325.642$, $df [6]$, $p < 0.001$). The DFA results were interpreted using pooled within-group correlations from the structure matrix (see Table 4). Loadings above 0.71 are considered excellent, 0.71- 0.63 are very good, 0.63-0.55 are good, 0.55-0.45 are fair, and below 0.45 are poor. In essence, the metric with the highest loading implies that this metric has a greater ability to discriminate between a CP and TD cycling pattern [32]. Using these criteria established by Comrey et al. [33], the pattern of correlations showed good loading from ArcL and DJ (0.576 and 0.545, respectively), while the remaining four metrics showed poor loadings. Because ArcL and DJ have the most contributions to the discriminant function, these variables have the most discriminatory abilities among the six smoothness metrics in identifying differences between different smoothness levels during cycling.

Table 4. Regression analysis summary for variables measuring cycling smoothness depicting the loadings for each metric in decreasing order, i.e., the metrics as listed from top to bottom as highest to lowest in their discriminatory ability between CP and TD cycling smoothness. Loadings above 0.71 are considered excellent, 0.71–0.63 are very good, 0.63–0.55 are good, 0.55–0.45 are fair, and below 0.45 are poor.

Variable	Within-Group Correlation
ArcL	0.576
DJ	0.545
RMSE	0.086
SALM	0.064
Xcorr	0.061
RI	0.045

Note: ArcL = arc length, SALM = spectral arc length of instant speed, RMSE = root mean square error from ideal cycling, XCorr = cross-correlation method, RI = roughness index, and DJ = dimensionless jerk.

The validity of our DFA analysis in discriminating between the TD and CP cycling patterns was evaluated through a classification analysis. The classification rate of 100% demonstrated that all participants in the CP and TD groups were correctly classified into either group based on the DFA results. This demonstrates the high accuracy of the DFA in predicting group membership.

4. Discussion

The objective of this study was to find the best metric to quantify CP cycling smoothness, using four previously proposed metrics, DJ, SALM, RI, and Xcorr, and two newly proposed metrics by our group, ArcL, and RMSE. To do so, first, we used a set of simulated signals, *crankSims*, with different levels of known un-smoothness by adding aberrant cycles. Thereby, we could visually inspect each metric's capability in differentiating between different levels of un-smoothness in a repeatable manner. The result of our analysis showed ArcL, DJ, and RMSE have the highest repeatability, i.e., less variability at each *crankSim* value, and can maintain an ascending trend. Secondly, to statistically quantify each metric's sensitivity in discriminating between a smooth and less smooth cycling motion, we performed DFA on the six metrics. Our results show that ArcL, with loading of 0.576 (within the good range), and demonstrating robustness in the repeatability evaluation, was the best metric in identifying unsmooth, halted cycling motion from smooth cycling. DJ, on the other hand, despite similar good loading, 0.545, did not show the same level of repeatability as ArcL.

ArcL vs. SALM. A desirable smoothness metric would be computationally inexpensive [14]. One of the outstanding characteristics of the ArcL is that it is not only computationally inexpensive but is also easily comprehensible and implementable. As the unsmoothness level increases, the length of the arc to reach the final crank angle, $N \times 360^\circ$, also increases. In the study by Balasubramanian et al. [12], the speed profile ArcL was also a reliable and sensitive metric to quantify upper extremity motion in healthy adults and the stroke population; however, SALM was outperforming their metric. Quijano-Gonzalez et al. also found that SALM was also the best metric to quantify upper extremity motion in the CP population [21]. One reason for the altered ranking of ArcL outperforming SALM in our study to the aforementioned studies is the nonexistence of submovement intervals in the *crankIS* motion signal we used. Balasubramanian et al. demonstrated that the sensitivity of the speed profile's ArcL decreases as the inter-submovement intervals increases in the intermittent upper extremity motion [12]. This sensitivity may also be the case for the position-based ArcL metric tested in our study. The manner in which we developed the *crankIS*, enabled us to eliminate the crank angles' submovements and to produce a continuous motion, which might contribute to the superior performance of the ArcL in quantifying cycling smoothness.

Temporal organization sensitivity. Balasubramanian et al. concluded that any metric could not be used on an entire rhythmic movement to estimate smoothness, because a candidate metric may be sensitive to the temporal organization of the motion [14]; e.g., changing the speed of a submovement and the length of the interval between each submovement can lead to disparate values for the similarly smooth signals. Note that, although cycling is continuous motion, the crank angle consists of multiple 0–360° crank rotations. Depending on the sensor used, e.g., if an absolute encoder is used, these rotations segment the motion into submovements, which together form a sawtooth signal. By generating the *crankIS* data for each trial, we eliminated sawtooth intermittency to alleviate the effect of the temporal organization by producing a continuously progressive crank angle signal. Alternatively, if an incremental encoder without a reference point is used to collect the crank angle signal, we will have this continuously progressive angle signal with the need for extra processing steps required for generating *crankIS*. *CrankIS* permits generating the three smoothness metrics, ArcL, XCorr, and RMSE. These three metrics have the capability of analyzing the entire movement sequence to capture smoothness in its entirety.

XCorr. Other metrics such as SALM and RI have been used to characterize smoothness of movement in upper limb motion. Xcorr showed promising results in differentiating between CP and TD cycling smoothness in the study by Sansare et al. [16]. Despite Xcorr showing merit in detecting smoothness levels when used independently, when the smoothness metrics were compared against each other, the ArcL accounted for the most between-group variance in the data and hence, was identified as the most sensitive measure.

Context-specific metrics. Because most cycling systems, like the one used in this study, have one degree of freedom, we could assume a subject-specific ideal scenario (*crankIDL*) for our cycling intervention, which matched the duration and number of revolutions of each subject. The *crankIDL* became closer to the physically achievable scenario after the elimination of the initial (acceleration) and the final (deceleration) revolutions. The existence of this ideal scenario enabled us to propose the XCorr and RMSE metrics. The ideal scenario might be difficult to assume in other contexts, such as gait smoothness, which limits the application of XCorr and RMSE. Additionally, in gait applications, ArcL may be more challenging to compute, as the increase in the prominence of peaks and valleys in some motion signals (e.g., shank angular velocity during gait) may be characteristics of desired motion, while it also increases the arc length of the signal. Thus, it would be hard to isolate the contribution of unsmooth motion from the more pronounced peaks and valleys in the signal. In contrast, SALM and DJ can be more universally used in various applications.

Limitations. Aside from the limited number of subjects included in our comparison, one of the major limitations of this study is that it only informs us about the ability of the metrics to distinguish between CP and TD cycling, where the differences in the smoothness levels might be more obvious compared to more subtle differences that might occur pre- and post-intervention. Even though the differentiation between CP and TD was not the objective of quantifying cycling smoothness, this differentiation was used because it is known that TD cycling is smoother than that of CP; this could be used as a benchmark to assess the strength of each metric to correctly detect such differences. Furthermore, because we recruited children aged 10–19 years, i.e., those at prepuberty, puberty, or postpuberty, it is possible that some developmental changes due to puberty stages may contribute to potential inter-group differences. Lastly, the habitual physical ability of the TD group may be higher than the CP group, and this may also contribute to some inter-group differences. While both these factors, i.e., changes due to puberty and habitual physical activity may affect cycling smoothness, it is beyond the scope of this study to address these contextual factors in-depth.

Implications, applications, and future directions. Despite the development of several smoothness metrics in recent years, there was a lack of a study that compared their performance on cycling motion. By analyzing the repeatability of the metrics on simulated data and the discriminatory ability of the metrics on CP and TD datasets, this study provides the first step in identifying a repeatable, sensitive metric for analyzing cycling smoothness in children with CP. Additionally, the results of this study can be extrapolated to other clinical populations (e.g., stroke) that have similar impairments such as spasticity, muscle co-contraction, and muscle weakness that might lead to unsmooth and halted cycling motion. While ArcL demonstrated the most promising repeatability and sensitivity with our dataset, future studies should look at its sensitivity in discriminating more subtle changes in smoothness such as pre- versus post-intervention improvements.

5. Conclusions

In our comparison of six metrics (DJ, SALM, RI, XCorr, which are previously proposed, and RMSE, and ArcL, which are proposed in this study), when visually inspected using simulated crank angles, ArcL, i.e., the length of the crank angle signal, demonstrated a high level of repeatability and sensitivity in differentiating decreasing levels of smoothness. DJ, a jerk-based metric, was the closest competitor. Both metrics, ArcL and DJ, showed a good level of sensitivity in differentiating TD and CP cycling. The proposed preprocessing technique in combination with ArcL may be used in future studies to quantify various levels of improvement in motor control post-cycling interventions.

Author Contributions: Conceptualization, A.B. and A.S.; methodology, A.B. and A.S.; software, A.B.; validation, A.B. and A.S.; formal analysis, A.S.; investigation, S.C.K.L.; resources, S.C.K.L.; data curation, S.C.K.L.; A.B writing—original draft preparation, A.B. and A.S.; writing—review and editing, S.C.K.L.; visualization, A.B.; supervision, S.C.K.L.; project administration, S.C.K.L.; funding acquisition, S.C.K.L. All authors have read and agreed to the published version of the manuscript.

Funding: This research was funded by the National Institutes of Health (NIH), grant number R01HD062588, Shriners Hospital for Children (Grant #8530), and a Clinical Research Grant from the Pediatric Section of the American Physical Therapy Association.

Institutional Review Board Statement: The study was conducted in accordance with the Declaration of Helsinki and approved by the Institutional Review Boards of Temple University and the University of Delaware (protocol code 11659).

Informed Consent Statement: Informed assent or consent (if 18 years old) was obtained from all subjects involved in the study, and a parent or legal guardian signed consent documents for minors. Written informed consent has been obtained from the patient(s) to publish this paper.

Data Availability Statement: The data presented in this study are available upon request from the corresponding author.

Conflicts of Interest: The authors declare no conflict of interest. The funders had no role in the design of the study; in the collection, analyses, or interpretation of data; in the writing of the manuscript; or in the decision to publish the results.

References

1. Bax, M.; Goldstein, M.; Rosenbaun, P.; Leviton, A.; Paneth, N.; Dan, B.; Jacobsson, B.; Damiano, D. Proposed definition and classification of cerebral palsy, April 2005. *Dev. Med. Child Neurol.* **2005**, *47*, 571. [[CrossRef](#)] [[PubMed](#)]
2. Wiley, M.E.; Damiano, D.L. Lower-extremity strength profiles in spastic cerebral palsy. *Dev. Med. Child Neurol.* **1998**, *40*, 100–107. [[CrossRef](#)] [[PubMed](#)]
3. Damiano, D.L.; Martellotta, T.L.; Sullivan, D.J.; Granata, K.P.; Abel, M.F. Muscle force production and functional performance in spastic cerebral palsy: Relationship of cocontraction. *Arch. Phys. Med. Rehabil.* **2000**, *81*, 895–900. [[CrossRef](#)] [[PubMed](#)]
4. Stackhouse, S.K.; Binder-Macleod, S.A.; Stackhouse, C.A.; McCarthy, J.J.; Prosser, L.A.; Lee, S.C. Neuromuscular electrical stimulation versus volitional isometric strength training in children with spastic diplegic cerebral palsy: A preliminary study. *Neurorehabil. Neural Repair* **2007**, *21*, 475–485. [[CrossRef](#)] [[PubMed](#)]
5. Stackhouse, S.K.; Binder-Macleod, S.A.; Lee, S.C.K. Voluntary muscle activation, contractile properties, and fatigability in children with and without cerebral palsy. *Muscle Nerve* **2005**, *31*, 594–601. [[CrossRef](#)] [[PubMed](#)]

6. Thelen, D.D.; Riewald, S.A.; Asakawa, D.S.; Sanger, T.D.; Delp, S.L. Abnormal coupling of knee and hip moments during maximal exertions in persons with cerebral palsy. *Muscle Nerve* **2003**, *27*, 486–493. [CrossRef]
7. Fujiwara, T.; Liu, M.; Chino, N. Effect of pedaling exercise on the hemiplegic lower limb. *Am. J. Phys. Med. Rehabil.* **2003**, *82*, 357–363. Available online: <https://journals.lww.com/> (accessed on 10 January 2020). [CrossRef] [PubMed]
8. Brown, D.A.; Nagpal, S.; Chi, S. Limb-loaded cycling program for locomotor intervention following stroke. *Phys. Ther.* **2005**, *85*, 159–168. [CrossRef]
9. Williams, H.; Pountney, T. Effects of a static bicycling programme on the functional ability of young people with cerebral palsy who are non-ambulant. *Dev. Med. Child Neurol.* **2007**, *49*, 522–527. [CrossRef]
10. Sejnowski, T.J. Making smooth moves. *Nature* **1998**, *394*, 725–726. [CrossRef]
11. Bosecker, C.; Dipietro, L.; Volpe, B.; Krebs, H.I. Kinematic Robot-Based Evaluation Scales and Clinical Counterparts to Measure Upper Limb Motor Performance in Patients With Chronic Stroke. *Neurorehabil. Neural Repair* **2010**, *24*, 62–69. [CrossRef]
12. Balasubramanian, S.; Melendez-Calderon, A.; Burdet, E. A robust and sensitive metric for quantifying movement smoothness. *IEEE Trans. Biomed. Eng.* **2012**, *59*, 2126–2136. [CrossRef] [PubMed]
13. Hogan, N.; Sternad, D. Sensitivity of Smoothness Measures to Movement Duration, Amplitude, and Arrests. *J. Mot. Behav.* **2009**, *41*, 529–534. [CrossRef]
14. Balasubramanian, S.; Melendez-Calderon, A.; Roby-Brami, A.; Burdet, E. On the analysis of movement smoothness. *J. Neuroeng. Rehabil.* **2015**, *12*, 112. [CrossRef] [PubMed]
15. Chen, H.Y.; Chen, S.C.; Chen, J.J.J.; Fu, L.L.; Wang, Y.L. Kinesiographical and kinematical analysis for stroke subjects with asymmetrical cycling movement patterns. *J. Electromyogr. Kinesiol.* **2005**, *15*, 587–595. [CrossRef]
16. Sansare, A.; Behboodi, A.; Johnston, T.E.; Bodt, B.; Lee, S.C.K. Characterizing Cycling Smoothness and Rhythm in Children With and Without Cerebral Palsy. *Front. Rehabil. Sci.* **2021**, *2*, 12. [CrossRef] [PubMed]
17. Ketcham, C.J.; Seidler, R.D.; Van Gemmert, A.W.A.; Stelmach, G.E. Age-related kinematic differences as influenced by task difficulty, target size, and movement amplitude. *J. Gerontol. Ser. B* **2002**, *57*, 54–64. [CrossRef]
18. Teulings, H.L.; Contreras-Vidal, J.L.; Stelmach, G.E.; Adler, C.H. Parkinsonism reduces coordination of fingers, wrist, and arm in fine motor control. *Exp. Neurol.* **1997**, *146*, 159–170. [CrossRef]
19. Smith, M.A.; Brandt, J.; Shadmehr, R. Motor disorder in Huntington’s disease begins as a dysfunction in error feedback control. *Nature* **2000**, *403*, 544–549. [CrossRef]
20. Platz, T.; Denzler, P.; Kaden, B.; Mauritz, K.H. Motor learning after recovery from hemiparesis. *Neuropsychologia* **1994**, *32*, 1209–1223. [CrossRef]
21. Montes, V.R.; Quijano, Y.; Chong Quero, J.E.; Ayala, D.V.; Perez Moreno, J.C. Comparison of 4 different smoothness metrics for the quantitative assessment of movement’s quality in the upper limb of subjects with cerebral palsy. In Proceedings of the Pan American Health Care Exchanges (PAHCE), IEEE Computer Society, Brasilia, Brazil, 7–12 April 2014.
22. Quijano-Gonzalez, Y.; Melendez-Calderon, A.; Burdet, E.; Chong-Quero, J.E.; Villanueva-Ayala, D.; Pérez-Moreno, J.C. Upper limb functional assessment of children with cerebral palsy using a sorting box. In Proceedings of the 2014 36th Annual International Conference of the IEEE Engineering in Medicine and Biology Society, EMBC 2014, Chicago, IL, USA, 26–30 August 2014; Institute of Electrical and Electronics Engineers Inc.: Piscataway, NJ, USA, 2014; pp. 2330–2333.
23. Anaya, L.; Quinones, I.; Quijano, Y.; Bueyes, V.; Chong, E.; Ponce, V. Clustering of Data that Quantify the Degree of Impairment of the Upper Limb in Patients with Alterations of the Central Nervous System. In Proceedings of the 2020 17th International Conference on Electrical Engineering, Computing Science and Automatic Control, CCE 2020, Mexico City, Mexico, 11–13 November 2020.
24. Chen, J.-J.J.; Chen, H.-Y.; Chen, S.-C.; Chen, C.-C. Clinical applications of FES-cycling to SCI and stroke subjects for smoother and symmetrical movement patterns. In Proceedings of the 11th Annual Conference of the International FES Society, Miyangi-Zao, Japan, 12–15 September 2006.
25. Lin, S.I.; Lo, C.C.; Lin, P.Y.; Chen, J.J.J. Biomechanical assessments of the effect of visual feedback on cycling for patients with stroke. *J. Electromyogr. Kinesiol.* **2012**, *22*, 582–588. [CrossRef]
26. Linder, S.M.; Rosenfeldt, A.B.; Bazyk, A.S.; Koop, M.M.; Ozinga, S.; Alberts, J.L. Improved lower extremity pedaling mechanics in individuals with stroke under maximal workloads. *Top. Stroke Rehabil.* **2018**, *25*, 248–255. [CrossRef] [PubMed]
27. Quian Quiroga, R.; Kraskov, A.; Kreuz, T.; Grassberger, P. Performance of different synchronization measures in real data: A case study on electroencephalographic signals. *Phys. Rev. E* **2002**, *65*, 14. [CrossRef] [PubMed]
28. Penney, G.P.; Weese, J.; Little, J.A.; Desmedt, P.; Hill, D.L. A comparison of similarity measures for use in 2-D-3-D medical image registration. *IEEE Trans. Med. Imaging* **1998**, *17*, 586–595. Available online: <https://ieeexplore.ieee.org/> (accessed on 10 January 2020). [CrossRef] [PubMed]
29. Palisano, R.; Rosenbaum, P.L.; Russell, D.; Galuppi, B.E. Development and reliability of a system to classify gross motor function in children with Cerebral Palsy ICF into Practice View project Development and initial validation of an assessment of visual ability for children with cerebral palsy View project. *Artic. Dev. Med. Child Neurol.* **1997**, *39*, 214–223. [CrossRef]
30. Sansare, A.; Harrington, A.T.; Wright, H.; Alesi, J.; Behboodi, A.; Verma, K.; Lee, S.C.K. Aerobic Responses to FES-Assisted and Volitional Cycling in Children with Cerebral Palsy. *Sensors* **2021**, *21*, 7590. [CrossRef] [PubMed]

31. Johnston, T.E.; Prosser, L.A.; Lee, S.C. Differences in pedal forces during recumbent cycling in adolescents with and without cerebral palsy. *Clin. Biomech.* **2008**, *23*, 248–251. Available online: <https://www.ncbi.nlm.nih.gov/> (accessed on 10 January 2020). [[CrossRef](#)]
32. Harrington, A.T.; McRae, C.G.A.; Lee, S.C.K. Evaluation of Functional Electrical Stimulation to Assist Cycling in Four Adolescents with Spastic Cerebral Palsy. *Int. J. Pediatr.* **2012**, *2012*, 1–11. [[CrossRef](#)]
33. Comrey, A.; Lee, H. *A First Course in Factor Analysis*, 2nd ed.; Psychology Press: New York, NY, USA, 1992.
34. Lachenbruch, P.A. An almost unbiased method of obtaining confidence intervals for the probability of misclassification in discriminant analysis. *Biometrics* **1967**, *23*, 639–645. [[CrossRef](#)]
35. Tabachnick, B.G.; Fidell, L.S. *Using Multivariate Statistics*, 7th ed.; Allyn & Bacon/Pearson Education: Boston, MA, USA, 2019; ISBN 978-0-13-479054-1.

Disclaimer/Publisher’s Note: The statements, opinions and data contained in all publications are solely those of the individual author(s) and contributor(s) and not of MDPI and/or the editor(s). MDPI and/or the editor(s) disclaim responsibility for any injury to people or property resulting from any ideas, methods, instructions or products referred to in the content.